The structure of isothermal, self-gravitating, stationary gas spheres for softened gravity

Jesper Sommer-Larsen[1], Henrik Vedel[1] and

Uffe Hellsten[2]

[1]Theoretical Astrophysics Center
Juliane Maries Vej 30, DK-2100 Copenhagen Ø, Denmark
(jslarsen@tac.dk, vedel@tac.dk)

[2]University of California, Lick Observatory,
Santa Cruz, CA 95064, USA
(uffe@ucolick.org)

Abstract

A theory for the structure of isothermal, self-gravitating gas spheres in pressure equilibrium is developed for softened gravity, assuming an ideal gas equation of state. The one-parameter spline softening proposed by Hernquist & Katz (1989) is used. We show that the addition of this extra scale-parameter implies that the set of equilibrium solutions constitute a one-parameter family, rather than the one and only one isothermal sphere solution for Newtonian

Submitted to the Astrophysical Journal

gravity.

We develop a number of approximate, analytical or semi-analytical solutions which apply in various regions of parameter space.

For softened gravity, the structure of isothermal spheres is, in general, very different from the Newtonian isothermal sphere. For example, as a corollary, we demonstrate the perhaps somewhat surprising result that even in the complete absence of rotational support it is possible, for *any* finite choice of softening length ϵ and temperature T, to deposit an arbitrarily large mass of gas in pressure equilibrium and with a non-singular density distribution inside of r_0 for *any* $r_0 > 0$ (neglecting effects of changes in the equation of state as well as general relativistic effects).

Furthermore, it is sometimes claimed that the size of the small scale, self-gravitating gas structures formed in dissipative Tree-SPH simulations is simply of the order the gravitational softening length. We demonstrate, that this, in general, is *not* correct.

The main purpose of the paper is to compare the theoretical predictions of our models with the properties of the small, massive, quasi-isothermal gas clumps ($r \sim 1$kpc, $M \sim 10^{10} M_{\odot}$ and $T \simeq 10^4 K$) which form in numerical Tree-SPH simulations of 'passive' galaxy formation of Milky Way sized galaxies (i.e. simulations not involving energy and momentum feedback to the gas from supernova explosions, stellar winds, UV radiation from OB stars etc.). We find reasonable agreement, despite the neglect of effects of rotational support in the models presented in this paper.

We comment on whether the hydrodynamical resolution is sufficient in our numerical simulations of galaxy formation involving highly super-sonic, radiative shocks and we give a necessary condition, in the form of a simple test, that the hydrodynamical resolution in any such simulations is sufficient.

Finally we conclude that one should be cautious, when comparing results of numerical simulations, involving gravitational softening and hydrodynamical smoothing, with reality.

1 Introduction

Due to the incredible increase in computing power provided by the computer industry over the last decade or so it has become possible to attempt to model, by 3-D numerical simulations, the formation and evolution of galaxies using various combinations of gravitational and hydrodynamical codes (e.g. Evrard 1988, Hernquist & Katz 1989, HK89 in the following). Since the physical problem involves very large density contrasts fully Lagrangian codes, like Tree-SPH (HK89) which is completely particle based, are particularly well suited for this problem. The Tree-SPH code calculates gravitational interactions using a hierarchical tree method (Barnes & Hut 1986) and the hydrodynamical interactions using the SPH (smoothed particle hydrodynamics) method (Lucy 1977; Gingold & Monaghan 1977).

Primarily to suppress effects of two-body gravitational interactions in such simulations the gravitational field of a gas or dark matter particles is softened, typically by using a Plummer softening kernel (Evrard 1988) or a spline softening kernel (HK89) - see section 2 for more details about gravitational softening.

In the 'passive' variant of such simulations (i.e. simulations not involving energy and momentum feedback to the interstellar medium due to supernova explosions, stellar winds, UV radiation from OB stars etc.) it is generally found that several small, massive gas clumps ($r \sim 1\mathrm{kpc}, m \sim 10^{10} M_{\odot}$ for simulations of Milky Way sized galaxies) are formed quite early in the simulations and survive for several Gyrs. The high density gas is nearly isothermal with a temperature $T \simeq 10^4 K$. This is due to the form of the radiative cooling function used in the simulations. The primordial gas cools quite effectively at temperatures $T \sim 10^4 - 10^6 K$, mainly through collisional excitation of H and He^+ by free electrons, but the cooling function is effectively truncated below $T \simeq 10^4 K$ where the density of free electrons rapidly tends to zero as the gas recombines. For low gas densities the radiative cooling can be suppressed, at the relevant temperatures $T \sim 10^4 - 10^6 K$, by up to two orders of magnitude by inclusion of effects of a background, ionizing, UVX radiation field, but at the high densities characteristic of the small, massive gas clumps the cooling function is essentially unchanged (Efstathiou 1992, Vedel, Hellsten & Sommer-Larsen 1994, VHSL94 in the following).

At first glance it seems somewhat surprising that such small, massive, isothermal gas clumps can be in quasi-equilibrium at a temperature of $T \simeq$

$10^4 K$, since for Newtonian gravity the mass inside of r of a stationary, isothermal, self-gravitating gas sphere is

$$m(< r) \lesssim \frac{2k_B T}{\mu m_p G}\, r = 3.2\ 10^7\ \frac{T_4}{\mu_{1.2}}\, r \quad M_\odot \quad , \tag{1}$$

where k_B is Boltzmann's constant, T the temperature, μ is the mean molecular weight, m_p is the proton mass, G is the gravitational constant, T_4 is the temperature in units of $10^4 K$, $\mu_{1.2}$ the mean molecular weight in units of 1.2 and r is in units of kpc in the last expression. Note, though, that, as shown by Ebert (1955) and Bonner (1956), the Newtonian isothermal sphere is only stable for

$$r < \ 1.72\ \sqrt{\frac{k_B T}{\mu m_p G \rho_0}}\ = 2.03\ r_{KING} = 1.21\ T_4^{0.5} \mu_{1.2}^{-0.5}\ n_0^{-0.5} \quad \text{kpc} \quad , \tag{2}$$

where ρ_0 is the central density, r_{KING} is given by equation (13) and n_0 is the central number density of hydrogen in units of cm^{-3}.

The dense, massive gas clumps are generally supported by rotation to some extent, but it is obviously of relevance to investigate whether such dense, massive gas clumps could be in equilibrium even in the absence of any rotational support at all, as a consequence of the gravitational softening. In the following it will be demonstrated that indeed they can.

In section 2 gravitational softening is briefly discussed. In section 3 pressure equilibrium solutions for isothermal, self-gravitating gas spheres will be derived for softened gravity. In section 4 the theoretical predictions will be discussed in relation to the results of numerical Tree-SPH simulations of galaxy formation. Section 5 constitutes the conclusion and finally in Appendix A the softened gravitational potential and gravitational field of an infinitely thin, spherical shell is determined.

2 Gravitational softening

One popular way of incorporating gravitational softening in numerical, particle based simulations is to replace the Newtonian potential, $\varphi(r) = -Gm/r$, of a point mass of mass m with the spherically symmetric Plummer potential $\varphi_P(r) = -Gm/\sqrt{r^2 + b^2}$, where b is the Plummer scale-parameter. From

Poissons equation it follows that the point mass is smeared out into a density distribution of total mass m

$$\rho_P(r) = \frac{3m}{4\pi b^3}(1 + \frac{r^2}{b^2})^{-5/2} \quad , \tag{3}$$

which is called the Plummer sphere - see e.g. Binney & Tremaine (1987). Note that, for $b > 0$, $\rho_P(r) > 0$ everywhere. This is to some extent a disadvantage, at least if the gravitational interactions are calculated with a Tree code - see the discussion in HK89.

HK89 proposed, inspired by the work of Gingold & Monaghan (1977), to soften the gravitational field of a point mass by using the same spline kernel as was used in their implementation of SPH. This spherically symmetric spline (softening) kernel, originally introduced by Monaghan & Lattanzio (1985), has the advantage that it has compact support at $r = 2\epsilon$, where the scale-parameter ϵ is denoted the softening length. The point mass of mass m is hence smeared out into a density distribution of total mass m

$$\rho_{spline}(r) = \frac{m}{\pi\epsilon^3} \begin{cases} 1 - 1.5u^2 + 0.75u^3 & 0 \leq u < 1 \\ 0.25\ (2-u)^3 & 1 \leq u < 2 \\ 0 & u \geq 2 \quad , \end{cases} \tag{4}$$

where $u = r/\epsilon$. Note that $\rho_{spline}(r) = 0$ for $u \geq 2$, so outside of $r = 2\epsilon$ the gravitational field and potential are exactly the same as for Newtonian gravity.

In our Tree-SPH simulations we use the HK89 spline softening for the reasons given above. We shall consequently adopt this type of gravitational softening in the following theoretical considerations also.

3 Equilibrium solutions for isothermal, self-gravitating gas spheres for softened gravity

We shall restrict the following analysis to spherically symmetric systems only:

The force equation for a stationary, isothermal, self-gravitating sphere gives

$$\frac{d\vec{u}}{dt} = -\frac{\nabla P}{\rho} - \nabla\varphi = \vec{0} \tag{5}$$

where $\vec{u}$ is the gas velocity, P the gas pressure, ρ the gas density and φ the gravitational potential.

Throughout this paper we assume that the hydrodynamics are described by the equations of ordinary gas physics.

In SPH the gas density (and effectively also all other hydrodynamical variables like gas pressure, energy, entropy etc.) is estimated on the basis of a smoothing kernel, which, for example, can be of the form given in equation (4) - see e.g. HK89 and references therein for further details. The characteristic smoothing scale is denoted the smoothing length h. When comparing the theoretical models, developed in the following, with the small, massive, quasi-isothermal gas clumps, formed in our Tree-SPH simulations, we assume, in this paper, that the theoretical predictions are directly applicable. This assumption is valid here, since h is always much smaller than the characteristic size of clumps. One should note, though, that this assumption will not always be valid.

Assuming an ideal gas equation of state

$$P = Nk_BT \tag{6}$$

where N is the gas number density, equations (5) and (6) yield for Newtonian gravity

$$\tilde{T}\frac{d\ln\rho}{dr} = -\frac{d\varphi}{dr} = -\frac{GM(r)}{r^2} \quad , \tag{7}$$

where

$$\tilde{T} = \frac{k_BT}{\mu m_p} = \gamma^{-1}c_s^2 \quad , \tag{8}$$

is a constant, since T in the following is assumed to be constant, and where γ is the adiabatic index, c_s the sound speed and

$$M(r) = 4\pi\int_0^r \rho(r')r'^2dr' \quad . \tag{9}$$

In equation (7) we use Newton's first and second theorems, that the gravitational acceleration $g(r)$ depends only on the *amount* of mass *inside* of r .

In the case of softened gravity the situation is very different: for a given softening length ϵ the softened gravitational acceleration $g_\epsilon(r)$ depends on the *density distribution* $\rho(r')$ for $r' \in [0, r + 2\epsilon]$, so in particular also on the density distribution out to two softening lengths *outside* of r.

As will be shown in the following, the change of the structure of isothermal spheres for softened gravity relative to the Newtonian case is, in general, quite dramatic.

For Newtonian gravity all solutions to equation (7) can be rescaled such that equation (7) effectively has one and only one solution in terms of the normalized density and radius

$$\tilde{\rho}_{KING}(\tilde{r}) = \frac{\rho(r)}{\rho_0} \quad , \tag{10}$$

where

$$\rho_0 = \rho(r = 0) \tag{11}$$

and

$$\tilde{r} = \frac{r}{r_{KING}} \tag{12}$$

and where

$$r_{KING} = \sqrt{\frac{9\tilde{T}}{4\pi G\rho_0}} = 0.595 \; T_4^{0.5} \; \mu_{1.2}^{-0.5} \; n_0^{-0.5} \;\; \text{kpc} \tag{13}$$

usually is denoted the King radius (e.g. Binney & Tremaine 1987).

In the case of softened gravity the gravitational field depends on one more parameter than for Newtonian gravity: ϵ, the softening length. One would consequently expect that all solutions to the force equation (7) can be rescaled in terms of a *one-parameter family* of solutions and, as we show in the following, this indeed is the case.

3.1 Scaling properties of the solutions

Let $(\epsilon, \tilde{T}, \rho_o)$ be given and let $\rho(r)$ be a solution to

$$\tilde{T}\frac{d\ln\rho}{dr} = -g_\epsilon(r) \quad , \tag{14}$$

where

$$g_\epsilon(r) = 4\pi \int_0^{r+2\epsilon} \tilde{g}_\epsilon(r, r')\rho(r')r'^2 dr' \tag{15}$$

and where $\tilde{g}_\epsilon(r, r')$ is the softened gravitational acceleration at r due to a unit mass, infinitely thin, spherical shell located at r'. In Appendix A an expression for $\tilde{g}_\epsilon(r, r')$ is derived.

It is straightforward to show that

$$\tilde{g}_{\epsilon'}(\alpha r, \alpha r') = \alpha^{-2}\tilde{g}_\epsilon(r, r') \quad , \tag{16}$$

where

$$\alpha = \frac{\epsilon'}{\epsilon} \quad . \tag{17}$$

Using this it is easy to show that, for parameters $(\epsilon' = \alpha\epsilon, \tilde{T}, \rho_0' = \alpha^{-2}\rho_0)$,

$$\rho'(r) = \alpha^{-2}\rho(\alpha^{-1}r) \tag{18}$$

is a solution to equation (14). In other words if we know all solutions to equation (14) for a given softening length ϵ, then all solutions, for *any* softening length $\epsilon' = \alpha\epsilon$, can be obtained by a mere scaling. Now, let again $(\epsilon, \tilde{T}, \rho_o)$ be given and let $\rho(r)$ be a solution to equation (14). It is straightforward to show that, for parameters $(\epsilon, \tilde{T}' = \beta\tilde{T}, \rho_0' = \beta\rho_0)$,

$$\rho'(r) = \beta\rho(r) \tag{19}$$

is a solution to equation (14). Again, if we know all solutions to equation (14) for a given value of $\tilde{T}$, then all solutions for *any* $\tilde{T}' = \beta\tilde{T}$ can be obtained by a mere scaling.

Consequently, in general, the solutions to equation (14) can be expressed as a one-parameter family in terms of a normalized density

$$\tilde{\rho}(r'; \rho_0') = \frac{\rho}{\rho_0} \quad , \tag{20}$$

where

$$r' = \alpha^{-1}r \tag{21}$$

and

$$\rho_0' = \alpha^2\beta^{-1}\rho_0 \quad . \tag{22}$$

3.2 The linear approximation and self-similarity

Fig. 1 shows the softened gravitational field, $g_\epsilon(r)$, for shells located at $u_{shell} = 0.0, 0.10, 0.30, 0.50$ and 1.00, where $u_{shell} = r_{shell}/\epsilon$. For $u_{shell} \lesssim 0.5$, the gravitational acceleration at $r \lesssim \epsilon/2$ due to such a shell is approximately linear in r:

$$g_\epsilon(r) \simeq -krM + O(r^3), \quad \text{for} \quad r \lesssim \epsilon/2 \quad \text{and} \quad r_{shell} \lesssim \epsilon/2 \quad , \tag{23}$$

where it follows from the Appendix of HK89 that the constant k is given by

$$k = \frac{4G}{3\epsilon^3} \quad . \tag{24}$$

Equation (14) can then be solved analytically assuming that the scale of the system is less than or comparable to $\epsilon/2$:

$$\rho(r) = \rho_0 \exp(-ar^2) \ , \quad \text{for} \quad r \lesssim \epsilon/2 \quad , \tag{25}$$

where

$$a = \frac{kM}{2\tilde{T}} \quad . \tag{26}$$

If, at $r \simeq \epsilon/2$, $\rho(r) << \rho_0$, then from the consistency relation for the total mass

$$M \simeq M_\infty = 4\pi\rho_0 \int_0^\infty \exp(-ar'^2) r'^2 dr' \quad , \tag{27}$$

it follows that

$$M \simeq 2\pi\rho_0 \Gamma(\frac{3}{2}) a^{-3/2} \quad . \tag{28}$$

M can then be obtained as

$$M \simeq M_{TAC} = (\frac{3\pi\tilde{T}\epsilon^3}{2G})^{3/5} \rho_0^{2/5} = 3.88 \ 10^8 \ T_4^{0.6} \ \mu_{1.2}^{-0.6} \ n_0^{0.4} \ \epsilon_3^{1.8} \quad M_\odot \quad , \tag{29}$$

where n is the number density of hydrogen in units of cm^{-3}, $n_0 = n(r = 0)$ and ϵ_3 is the softening length in units of 3 kpc.

From equations (24), (26) and (29) it follows that

$$a = (\frac{2}{3})^{2/5} \ \pi^{3/5} \ G^{2/5} \ \tilde{T}^{-2/5} \ \epsilon^{-6/5} \ \rho_0^{2/5} \quad . \tag{30}$$

We now introduce the characteristic length scale r_{TAC}:

$$r_{TAC} = 3\ (2a)^{-1/2} = \ 2.74\ T_4^{0.2}\ \mu_{1.2}^{-0.2}\ \epsilon_3^{0.6}\ n_0^{-0.2}\ \ \text{kpc}\ \ . \tag{31}$$

Equation (25) can then be rewritten as

$$\rho_{TAC}(r) = \rho_0 \exp(-(\frac{r^2}{2(r_{TAC}/3)^2}))\ \ , \tag{32}$$

or as

$$\tilde{\rho}_{TAC}(\tilde{r}) = \frac{\rho}{\rho_0} = \exp(-4.5\tilde{r}^2)\ \ , \tag{33}$$

where $\tilde{r} = r/r_{TAC}$. Hence the density distribution is gaussian in r with dispersion $r_{TAC}/3$. So for $r_{TAC} << \epsilon$ all solutions can be rescaled in terms of one and only one solution, as is the case for the Newtonian isothermal sphere, though the nature of the two solutions is very different.

It is sometimes claimed that the size of the small scale, self-gravitating gas structures formed in dissipative Tree-SPH simulations is simply of the order the gravitational softening length. From equation (31) it follows that, in general, this is *not* correct.

3.3 The point mass approximation

From Fig. 1 it can be seen that, for a given softening length ϵ and a shell of mass m located at $r_{shell} \lesssim \epsilon/2$, a point mass of mass m at $r' = 0$ results in a softened gravitational field, which is a quite good approximation to softened gravitational field of the shell and for $r \gtrsim \epsilon/2$ is a significantly better approximation, than the linear approximation discussed in the previous section.

Rewriting equation (14) as

$$\tilde{T}\frac{d\ln\rho}{dr} = -M\frac{d\varphi_{pm}}{dr}\ \ , \tag{34}$$

where φ_{pm} is the specific potential corresponding to the softened gravitational field of a point mass of unit mass, it follows by integration of equation (34) that $\rho_{pm}(r)$ can be expressed as

$$\rho_{pm}(r) = \rho_0 \exp(-(\varphi_{pm}(r) - \varphi_{pm}(r=0))\frac{M}{\tilde{T}})\ \ . \tag{35}$$

In the Appendix of HK89 $\varphi_{pm}(r)$ is expressed as

$$\varphi_{pm}(r) = -Gf(r) \ ; \tag{36}$$

the function $f(r)$ is also given as equation (A3) in Appendix A of this paper.

Equation (34) can hence be rewritten as

$$\tilde{\rho}_{pm} = \frac{\rho}{\rho_0} = \exp((f(r) - f(r=0)) \ \frac{GM}{\tilde{T}}) \ . \tag{37}$$

The consistency equation for the total mass can not be used in this case, since it can be shown that

$$M(r) = 4\pi\rho_0 \int_0^r \rho_{pm}(r') r'^2 dr' \rightarrow \infty \text{ as } r \rightarrow \infty \ . \tag{38}$$

However, by setting $M = M_{TAC}$ in equation (37), one obtains, for systems characterized by $r_{TAC} \lesssim \epsilon$, a generally much better approximation to the true solution than for the linear approximation - see the following subsection.

3.4 The general solution

A numerical, iterative algorithm was developed to obtain exact solutions of equation (14).

The general solutions can conveniently be expressed as

$$\tilde{\rho}(u; u_{TAC}) = \frac{\rho}{\rho_0} \ , \tag{39}$$

where $u = r/\epsilon$ and

$$u_{TAC} = \frac{r_{TAC}}{\epsilon} = 0.913 \ T_4^{0.2} \ \mu_{1.2}^{-0.2} \ \epsilon_3^{-0.4} \ n_0^{-0.2} \ . \tag{40}$$

In Fig. 2 the solutions are shown, as functions of u, for a large range of the u_{TAC} parameter. As $u_{TAC} \rightarrow 0$ the solutions, as functions of u, converge towards a vertical line at $r = 0$ and as $u_{TAC} \rightarrow \infty$ the solutions, as functions of u, converge towards a horizontal line at $\tilde{\rho} = 1$.

As $u_{TAC} \rightarrow 0$, then r_{TAC} becomes the characteristic linear scale of the isothermal spheres and the solutions converge as

$$\tilde{\rho}(u; u_{TAC}) \rightarrow \tilde{\rho}_{TAC}(u/u_{TAC}) \ , \qquad u_{TAC} \rightarrow 0 \ . \tag{41}$$

Conversely, as $u_{TAC} \rightarrow \infty$ r_{KING} becomes the characteristic linear scale of the isothermal spheres and the solutions converge as

$$\tilde{\rho}(u; u_{TAC}) \rightarrow \tilde{\rho}_{KING}(u/u_{KING}) \ , \qquad u_{TAC} \rightarrow \infty \ , \tag{42}$$

where $u_{KING} = r_{KING}/\epsilon$ and there is a one-to-one relation between u_{KING} and u_{TAC}:

$$u_{KING} = 0.249 \ u_{TAC}^{2.5} \ . \tag{43}$$

In Fig.3 $\tilde{\rho}/\tilde{\rho}_{TAC}$ is shown, as function of r/r_{TAC}, for various values of u_{TAC} and, as expected, $\tilde{\rho}/\tilde{\rho}_{TAC} \rightarrow 1$ as $u_{TAC} \rightarrow 0$.

In Fig.4 $\tilde{\rho}/\tilde{\rho}_{KING}$ is shown, as function of r/r_{KING}, for various values of u_{TAC} and, likewise as expected, $\tilde{\rho}/\tilde{\rho}_{KING} \rightarrow 1$ as $u_{TAC} \rightarrow \infty$.

In Fig. 5 $\tilde{\rho}/\tilde{\rho}_{pm}$ is shown, as a function of r/r_{TAC}, for various values of u_{TAC} and, as can be seen from the figure, $\tilde{\rho}/\tilde{\rho}_{pm} \rightarrow 1$ as $u_{TAC} \rightarrow 0$ - as expected - and it is obvious that the point mass approximation, in general, is much better than the linear approximation (Fig. 3), as discussed in subsection 3.3.

Fig. 6 shows M/M_{TAC} as a function of $u = r/\epsilon$ for various values of u_{TAC}. As can be seen from the figure, $M \simeq M_{TAC}$ for $u_{TAC} \lesssim 0.5$ whereas for larger values of u_{TAC}, M becomes increasingly larger than M_{TAC} and increases steadily with u.

This behaviour is expected, since for $u_{TAC} \gtrsim 0.5$ the linear approximation breaks down and for the point mass approximation, for the general solution and for the Newtonian isothermal sphere it can be shown that $M(u) \rightarrow \infty$ as $u \rightarrow \infty$.

Fig. 7 shows, for $\epsilon = 3$ kpc, a typical value used in current Tree-SPH simulations of galaxy formation, and $(T_4/\mu_{1.2}) = 1$, the density profiles of the general solution for $\log(n_0)$ = -2, -1, ... , 6. Similarly Fig. 8 shows, for the same parameters, $M(r)$ in units of $10^8 M_\odot$.

As can be seen, the masses are in general much larger, at $r \sim 1$ kpc, which is the typical size of the massive, cold gas clumps formed in our 'passive' simulations, than would be expected on the basis of isothermal sphere solutions for Newtonian gravity - see equation (1).

As a corollary it follows from equations (29) and (31) that, for given physical parameters $(\epsilon, \tilde{T})$, $r_{TAC} \rightarrow 0$ and $M_{TAC} \rightarrow \infty$ as $n_0 \rightarrow \infty$. So we obtain the perhaps somewhat surprising result that for *any* $\epsilon > 0$ and *any* positive value of $(T_4/\mu_{1.2})$ - like $\simeq 1$ for typical small, massive, cold clumps

formed in Tree-SPH simulations of 'passive' galaxy formation - it is possible to deposit an arbitrarily large mass of gas in pressure equilibrium and with a non-singular density distribution inside of r_0, for *any* $r_0 > 0$ (neglecting effects of changes in the equation of state as well as general relativistic effects).

4 Comparing with the results of numerical Tree-SPH simulations

To compare the theoretical predictions obtained in the previous section with what is actually found in numerical Tree-SPH simulations of 'passive' galaxy formation, we performed a series of simulations, starting from vacuum boundary, top-hat initial conditions, similar to those described in VHSL94. These simulations are not very realistic with regards to galaxy formation, but this is of no consequence for the present purpose.

We carried out four simulations. The first three only differed by having $\epsilon_{SPH} = 1.5$, 3.0 and 6.0 kpc respectively. The fourth was a higher resolution simulation - it was identical to the second simulation except that 8 times more gas particles (each with one eighth of the original gas particle mass) were used (but note that *no* extra phases were added to the initial conditions). The purpose of this simulation was to check whether the hydrodynamical resolution was sufficient in our simulations. Other details about the simulations are given in Table 1.

In each of the four simulations we selected the three most massive, cold gas clumps ($(T_4/\mu_{1.2}) \simeq 1$) at time $t = 3.2$ Gyr. At this time all the cold gas clumps were self-gravitating. They typically form at $t \lesssim 1$ Gyr in 'mini' dark matter halos, but the dark matter is stripped off during the violent relaxation phase at first recollapse of the proto-galaxy at $t \simeq 2.2$ Gyr.

All the cold gas clumps had, at $t = 3.2$ Gyr, a radial extent of less than or order ϵ. The cumulative mass distribution, at $t = 3.2$ Gyr, for the largest, cold gas clump in simulations #1-3, is shown in Fig. 9 and the cumulative mass distribution, at $t = 3.2$ Gyr, for simulations #2 and #4 (low versus high hydrodynamical resolution), is shown in Fig. 10 for all three clumps.

For each cold gas clump we measured the mass M_{obs} and the central density n_0 and determined the mass M_{teo}, which would be expected for an

isothermal sphere of this central density and parameters ϵ_3 and $(T_4/\mu_{1.2})$ as in the simulations (all gas clumps were in the $u_{TAC} \lesssim 1$ regime). The ratio M_{teo}/M_{obs} for the individual clumps is plotted in Fig. 11. As can be seen from the figure, M_{teo}/M_{obs} is generally well below unity, indicating that effects of rotational support, which are not included in our theoretical models, is of importance. For all the clumps M_{teo}/M_{obs} is observed to increase as ϵ increases. This is to be expected since, for clumps of similar mass and specific angular momentum, the ratio q of pressure force to total gravitational force scales approximately as $\epsilon^{3/2}$ when q is well below unity and $u_{TAC} \lesssim 1$. Furthermore, as the clump masses decrease, M_{teo}/M_{obs} is observed to increase for a given ϵ. This is also to be expected, though on rather more complicated grounds: Theoretically one would expect that the average dimensionless spin-parameter $< \lambda >$ depends only weakly on the magnitude of the initial density fluctuations later collapsing and forming the 'mini' dark matter halos in which the gas clumps subsequently form dissipatively (e.g. Barnes & Efstathiou 1987). If one furthermore assumes that the mass of a gas clump depends on the circular speed v_c of its 'mini' dark matter halo like $M \propto v_c^{\alpha},\ \alpha \simeq 3$, from e.g. the Tully-Fisher relation, then one can show that, for a given softening length, q scales approximately as M^{-2} for q well below unity and $u_{TAC} \lesssim 1$.

For the smallest clump in simulations #1-4 the effect of pressure forces appears to be comparable to the effect of rotational support. In fact, for softened gravity, the relationship between the physical structure of self-gravitating, rotationally supported systems and the gravitational softening length ϵ is quite similar to what is found in this paper for isothermal spheres, as shown in Sommer-Larsen, Vedel & Hellsten (1997).

Finally a note on hydrodynamical resolution in Tree-SPH simulations: From Figs. 10 and 11 it seems - comparing simulations #2 and #4 - that the hydrodynamical resolution is sufficient. At later times, when the clumps have merged and super-sonic, radiative shocks have occurred, the results of simulations #2 and #4 are still very similar - as an example the surface density in the resulting gas disks, at $t = 5.2$ Gyr, is shown in Fig. 12 for simulations #2 and #4. This is quite reassuring, because, whereas in nonradiative shocks the density contrast always is less than the Rankine-Hugoniot limit of $(\frac{\gamma+1}{\gamma-1})$, where γ is the adiabatic index, significantly larger density contrasts most probably occur in the radiative shocks and this could potentially cause spurious effects, because of effects of limited shock resolution due to

the smoothing, inherent in SPH.

We propose that one should always test a SPH simulation in the manner described above for simulations #2 and #4. Such a simple test constitutes a necessary (but not, in general, sufficient) condition that the hydrodynamical resolution is sufficiently high to adequately resolve super-sonic, radiative shocks.

5 Conclusion

We have developed a theory for the structure of isothermal, self-gravitating gas spheres in pressure equilibrium for softened gravity, based on the spline softening kernel proposed by Hernquist & Katz (1989).

Because the gravitational force depends on an extra scale-parameter, the softening length ϵ, relative to Newtonian gravity, the solutions constitute a one-parameter family, rather than the one and only one isothermal sphere solution for Newtonian gravity.

For softened gravity the structure of isothermal spheres is, in general, very different from the Newtonian, isothermal sphere.

For example we find, as a corollary, the perhaps somewhat surprising result, that, for *any* finite softening length ϵ and temperature T, it is possible to deposit an arbitrarily large mass of gas, in pressure equilibrium and with a non-singular density distribution, inside of r_0, for *any* $r_0 > 0$ (neglecting effects of changes in the equation of state and general relativistic effects).

Furthermore, it is sometimes claimed that the size of the small scale, self-gravitating gas structures formed in dissipative Tree-SPH simulations is simply of the order the gravitational softening length. We demonstrate, that this, in general, is *not* correct.

The main purpose of the paper is to compare the theoretical predictions of our models with the properties of the small, massive, quasi-isothermal gas clumps formed in numerical Tree-SPH simulations of 'passive' galaxy formation of Milky Way sized galaxies (i.e. simulations not involving energy and momentum feedback to the gas from supernova explosions, stellar winds, UV radiation from OB stars etc.). We find reasonable agreement, despite the neglect of effects of rotational support in our theoretical models.

We would expect that if the gravitational softening was based on a Plummer kernel (which is also a one scale-parameter type of softening), rather than

the spline kernel, the resulting isothermal spheres would be qualitatively similar to those described in this paper. We encourage any Plummer softening 'fan' to check this quantitatively by going through a similar exercise as described in this paper for the spline softening.

We have not discussed the stability of the isothermal sphere equilibrium solutions obtained in this work - we shall return to this issue in a forthcoming paper using an approach similar to that outlined by Ebert (1955) and Bonner (1956).

We comment on whether the hydrodynamical resolution is sufficient in our numerical simulations of galaxy formation involving highly super-sonic, radiative shocks and we give a necessary condition, in the form of a simple test, that the hydrodynamical resolution in any such simulations is sufficient.

The results obtained in this paper, and in Sommer-Larsen, Vedel & Hellsten (1997), seem to indicate that one should be cautious when comparing what is observed in the real Universe with results of numerical Tree-SPH simulations or any other numerical, gravitational-hydrodynamical simulations, where the calculation of the gravitational interactions, locally or globally, is particle based and the gravitational field of the individual particles is softened.

To summarize: Without proper testing/understanding of the effects of gravitational softening and hydrodynamical smoothing in numerical gravitational-hydrodynamical simulations of various physical problems, the degree of reality represented by such simulations may be quite difficult to assess.

Acknowledgements

We have benefitted considerably from discussions with Cedric Lacey and Draza Marković. This work was supported by Danmarks Grundforskningsfond through its support for an establishment of the Theoretical Astrophysics Center. UH acknowledges support by a postdoctoral research grant from the Danish Natural Science Research Council.

References

Barnes, J., Efstathiou, G., 1987, ApJ, 319, 575

Barnes, J., Hut, P., 1986, Nature, 324, 446

Binney, J., Tremaine, S., 1987, Galactic Dynamics. Princeton Univ. Press, Princeton

Bonner, W.B., 1956, MNRAS, 116, 351

Ebert, R., 1955, Zs.Ap., 37, 217

Efstathiou, G., 1992, MNRAS, 43p

Evrard, A.E., 1988, MNRAS, 235, 911

Gingold, R.A., Monaghan, J.J., 1977, MNRAS, 181, 375

Hernquist, L., Katz, N., 1989, ApJS, 70, 419 (HK89)

Lucy, L., 1977, AJ, 82, 1013

Monaghan, J.J., Lattanzio, J.C., 1985, A&A, 149, 135

Sommer-Larsen, J., Vedel, H., Hellsten, U., 1997, in preparation

Vedel, H., Hellsten, U., Sommer-Larsen, J., 1994, MNRAS, 271, 743 (VHSL94)

Appendix A: The softened gravitational potential and gravitational field of an infinitely thin, spherical shell

It is fairly easy to show that the potential, at radial coordinate r, of an infinitely thin, spherical shell with radius R and unit mass is given by

$$\varphi_{shell}(r,R) = \begin{cases} \frac{1}{2Rr}\int_{R-r}^{R+r}\varphi_{pm}(r')r'dr' \ , & r < R \\ \\ \frac{1}{2Rr}\int_{r-R}^{r+R}\varphi_{pm}(r')r'dr' \ , & r \geq R \end{cases} \tag{A1}$$

where φ_{pm} is the softened potential of a point mass of unit mass. In the Appendix of HK89 φ_{pm} is expressed as

$$\varphi_{pm}(r) = -Gf(r) \ , \tag{A2}$$

where

$$f(r) = \begin{cases} -[2u^2/3 - 3u^4/10 + u^5/10]/\epsilon + 1.4/\epsilon & 0 \leq u < 1 \\ -1/(15r) - [4u^2/3 - u^3 + 3u^4/10 - u^5/30]/\epsilon + 1.6/\epsilon & 1 \leq u < 2 \\ 1/r & u \geq 2 \end{cases} \tag{A3}$$

The gravitational acceleration, at r, from the unit mass shell at R, is then given by

$$\tilde{g}_\epsilon(r,R) = \ -\ d\varphi_{shell}/dr = \tag{A4}$$

$$\begin{array}{ll} \frac{1}{2Rr^2}\int_{R-r}^{R+r}\varphi_{pm}(r')r'dr' & \\ -\frac{1}{2R}(\varphi_{pm}(R+r) - \varphi_{pm}(R-r)) & \\ -\frac{1}{2r}(\varphi_{pm}(R+r) + \varphi_{pm}(R-r)) & r < R \ , \end{array}$$

and

$$\begin{array}{ll} \frac{1}{2Rr^2}\int_{r-R}^{r+R}\varphi_{pm}(r')r'dr' & \\ -\frac{1}{2R}(\varphi_{pm}(r+R)-\varphi_{pm}(r-R)) & \\ -\frac{1}{2r}(\varphi_{pm}(r+R)+\varphi_{pm}(r+R)) & r \geq R\ . \end{array}$$

It is possible to calculate $\tilde{g}_\epsilon(r,R)$ analytically, but as the result is quite complicated and voluminous, we shall omit it here.

From equation (A4) it follows that for a spherical system, with mass distribution $\rho(r)$, the gravitational acceleration at r is given by

$$g_\epsilon(r) = 4\pi \int_0^{r+2\epsilon} \tilde{g}_\epsilon(r,r')\rho(r')r'^2 dr' \quad . \tag{A5}$$

Figure captions

Figure 1: Gravitational acceleration due to infinitely thin, spherical shells of mass m located at $u_{shell} = r_{shell}/\epsilon = 0.00$, 0.10, 0.33, 0.50 and 1.00. Solid line corresponds to $u_{shell} = 0.00$ and as u_{shell} increases the curves move monotonically upwards. The linear approximation is shown as the straight dotted line.

Figure 2: The general solutions for isothermal spheres for softened gravity. As u_{TAC} increases the solutions become monotonically more horizontal.

Figure 3: ρ/ρ_{TAC} as a function of r/r_{TAC}. The solid, horizontal, straight line corresponds to $u_{TAC} = 0.00$. As u_{TAC} increases the curves move monotonically towards the other solid line, which represents $u_{TAC} = \infty$.

Figure 4: ρ/ρ_{KING} as a function of r/r_{KING}. As u_{TAC} increases the curves converge towards the solid, horizontal, straight line, which corresponds to $u_{TAC} = \infty$. The other solid line corresponds to $u_{TAC} = 0.00$.

Figure 5: ρ/ρ_{pm} as a function of r/r_{TAC}. As u_{TAC} decreases the curves converge towards the solid, horizontal, straight line, which corresponds to $u_{TAC} = 0.00$

Figure 6: M/M_{TAC} as a function of r/ϵ. As u_{TAC} increases the curves start out monotonically less steep.

Figure 7: Density distributions for isothermal spheres, of various central hydrogen number density n_0, for $T = 10^4$ K and gravitational softening length $\epsilon = 3.0$ kpc.

Figure 8: Cumulative mass distribution for isothermal spheres, of various central hydrogen number density n_0, for $T = 10^4$ K and gravitational softening length $\epsilon = 3.0$ kpc. The lines correspond to the same values of n_0 as in Fig. 7.

Figure 9: Cumulative mass distribution, at $t = 3.2$ Gyr, for the most massive, cold gas clump in simulations #1-3.

Figure 10: Cumulative mass distribution, at $t = 3.2$ Gyr, for the three most massive, cold gas clumps in simulations #2 and #4.

Figure 11: The ratio of the theoretical to observed mass, at $t = 3.2$ Gyr, for the three most massive, cold gas clumps in simulations #1-4. For more details - see text.

Figure 12: The gas surface density distributions, at $t = 5.2$ Gyr, for the disks formed in simulations #2 and #4.

Table 1: Tree-SPH simulations #1-4.

Simulation	ϵ_{SPH}	ϵ_{DM}	N_{SPH}	N_{DM}
	[kpc]	[kpc]		
#1	1.5	10.0	2048	2048
#2	3.0	10.0	2048	2048
#3	6.0	10.0	2048	2048
#4	3.0	10.0	16384	2048

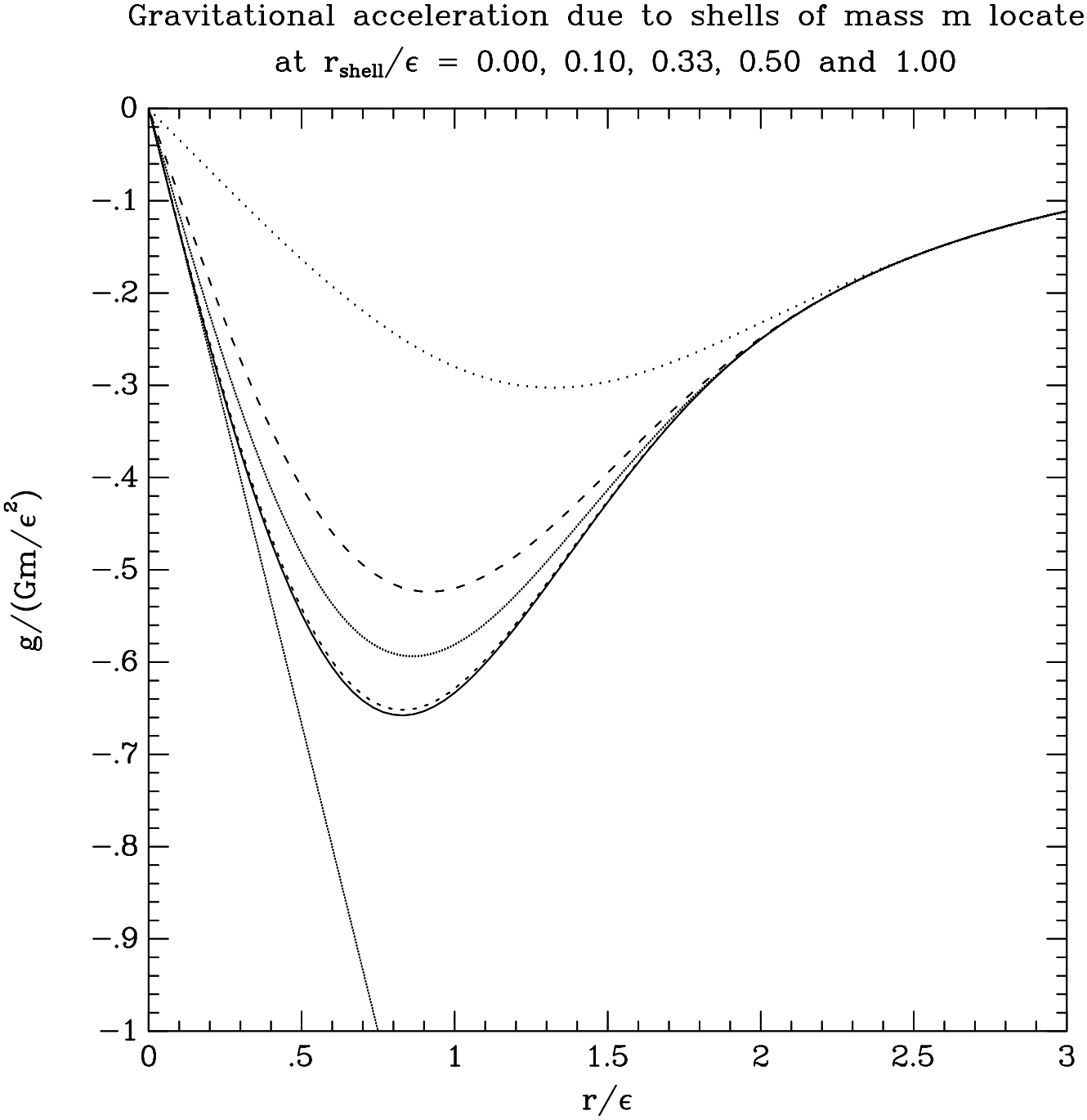
Gravitational acceleration due to shells of mass m located
at r_{shell}/ϵ = 0.00, 0.10, 0.33, 0.50 and 1.00
0
−.1
−.2
−.3
−.4
−.5
−.6
−.7
−.8
−.9
−1
$g/(Gm/\epsilon^2)$
0
.5
1
1.5
2
2.5
3
r/ϵ

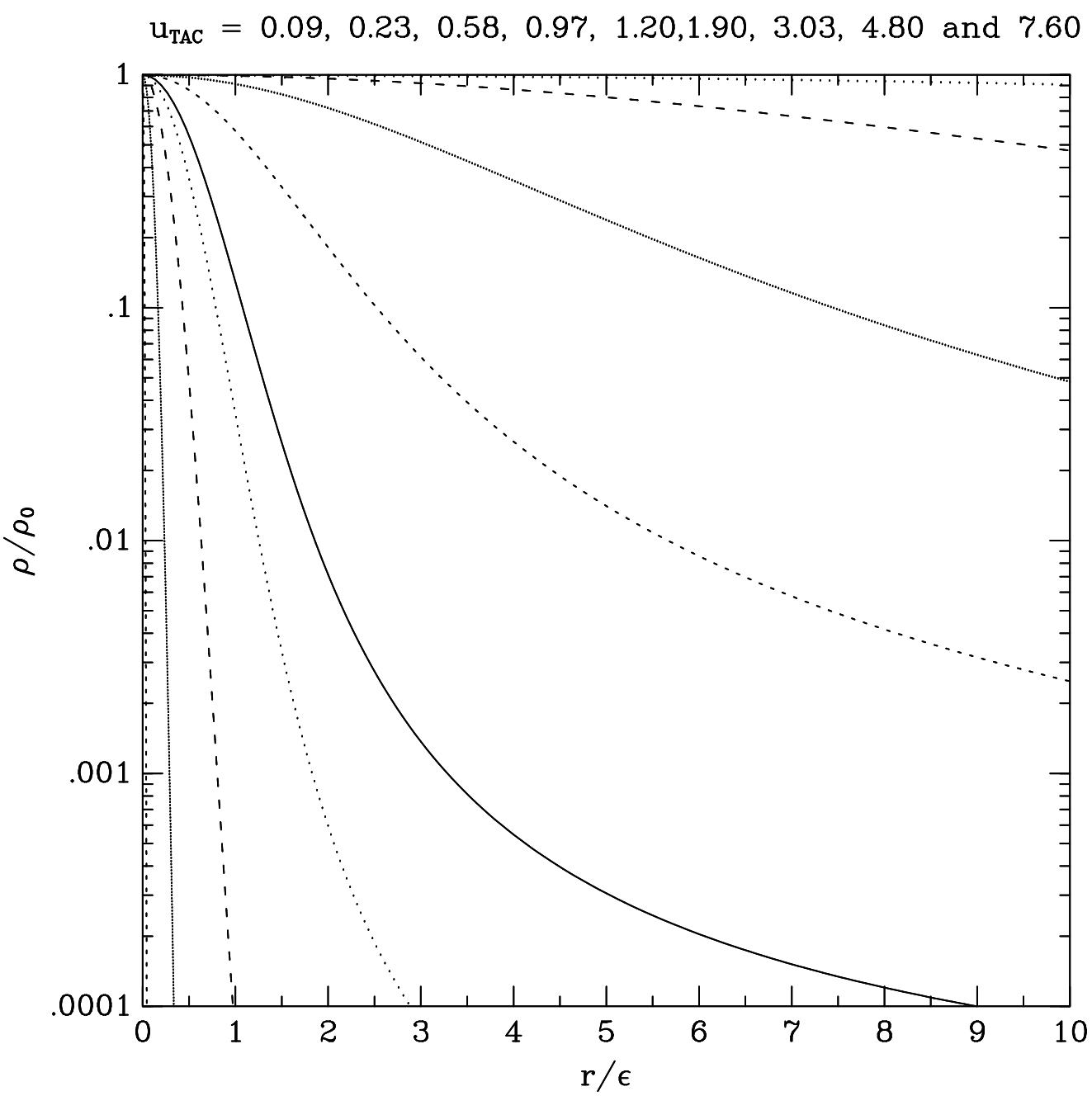
u_{TAC} = 0.09, 0.23, 0.58, 0.97, 1.20,1.90, 3.03, 4.80 and 7.60
1
.1
.01
.001
.0001
ρ/ρ_0
0
1
2
3
4
5
6
7
8
9
10
r/ϵ

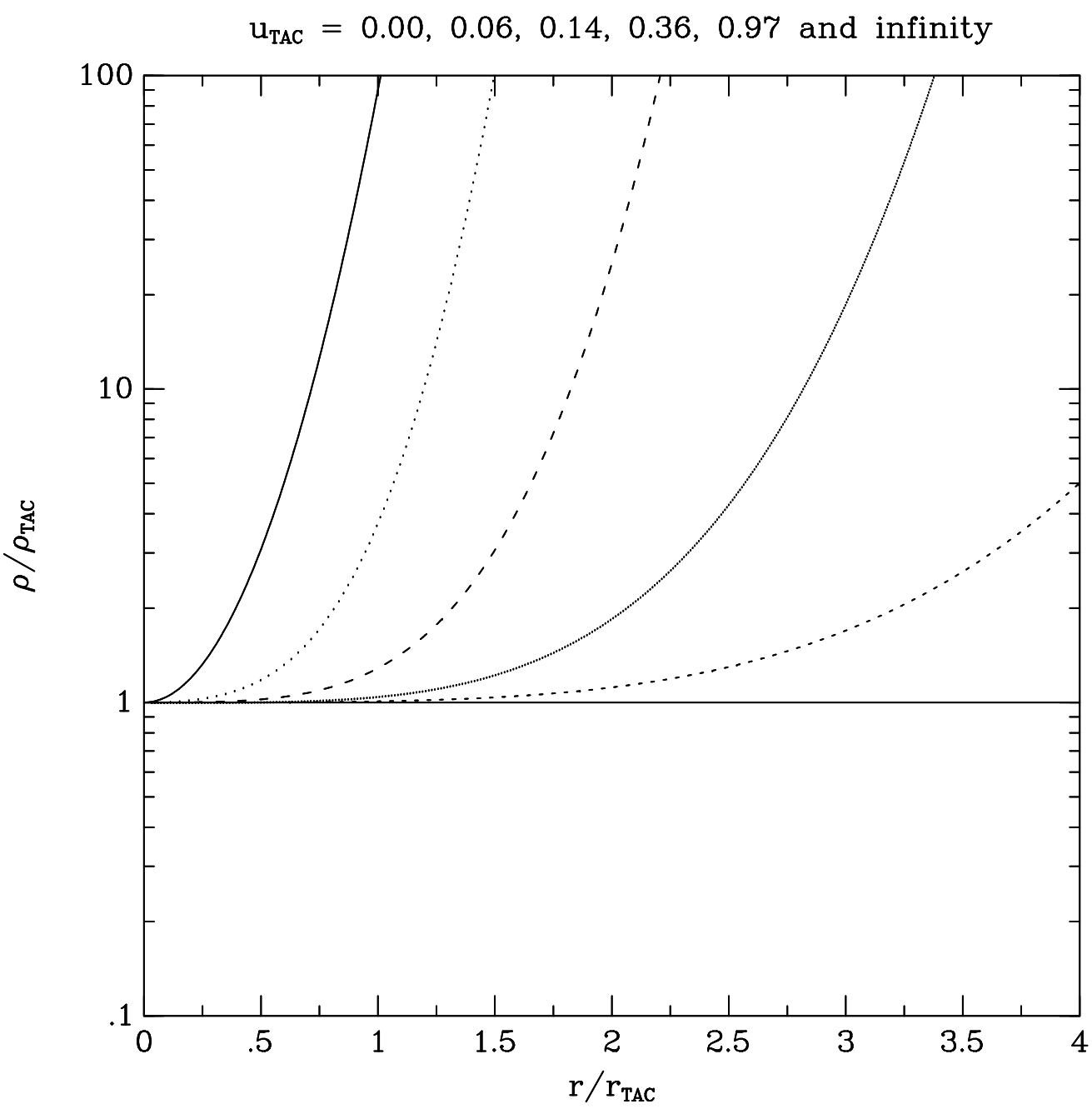
u_{TAC} = 0.00, 0.06, 0.14, 0.36, 0.97 and infinity
100
10
1
.1
ρ/ρ_{TAC}
0
.5
1
1.5
2
2.5
3
3.5
4
r/r_{TAC}

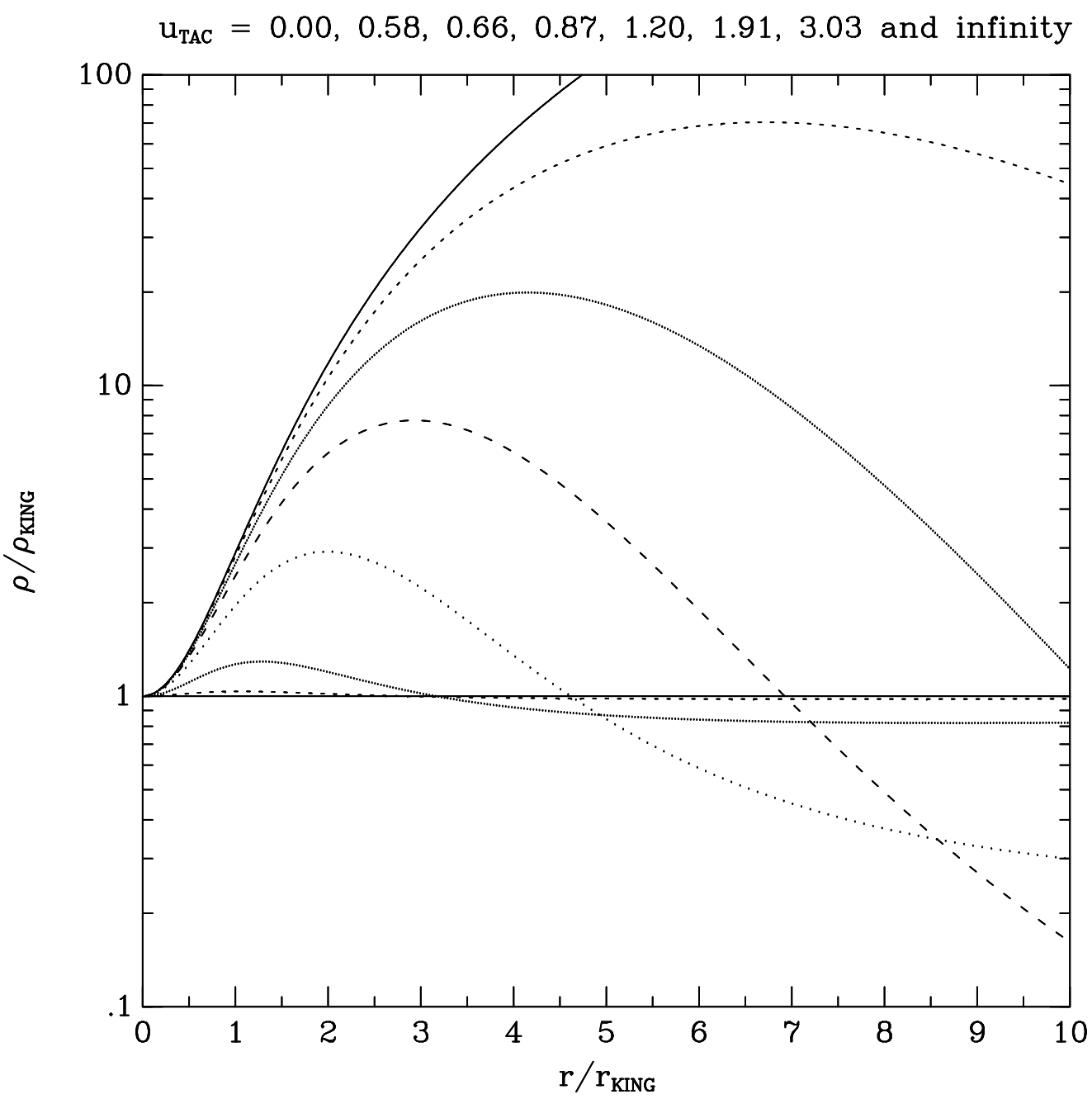
u_{TAC} = 0.00, 0.58, 0.66, 0.87, 1.20, 1.91, 3.03 and infinity
100
10
1
.1
ρ/ρ_{KING}
0
1
2
3
4
5
6
7
8
9
10
r/r_{KING}

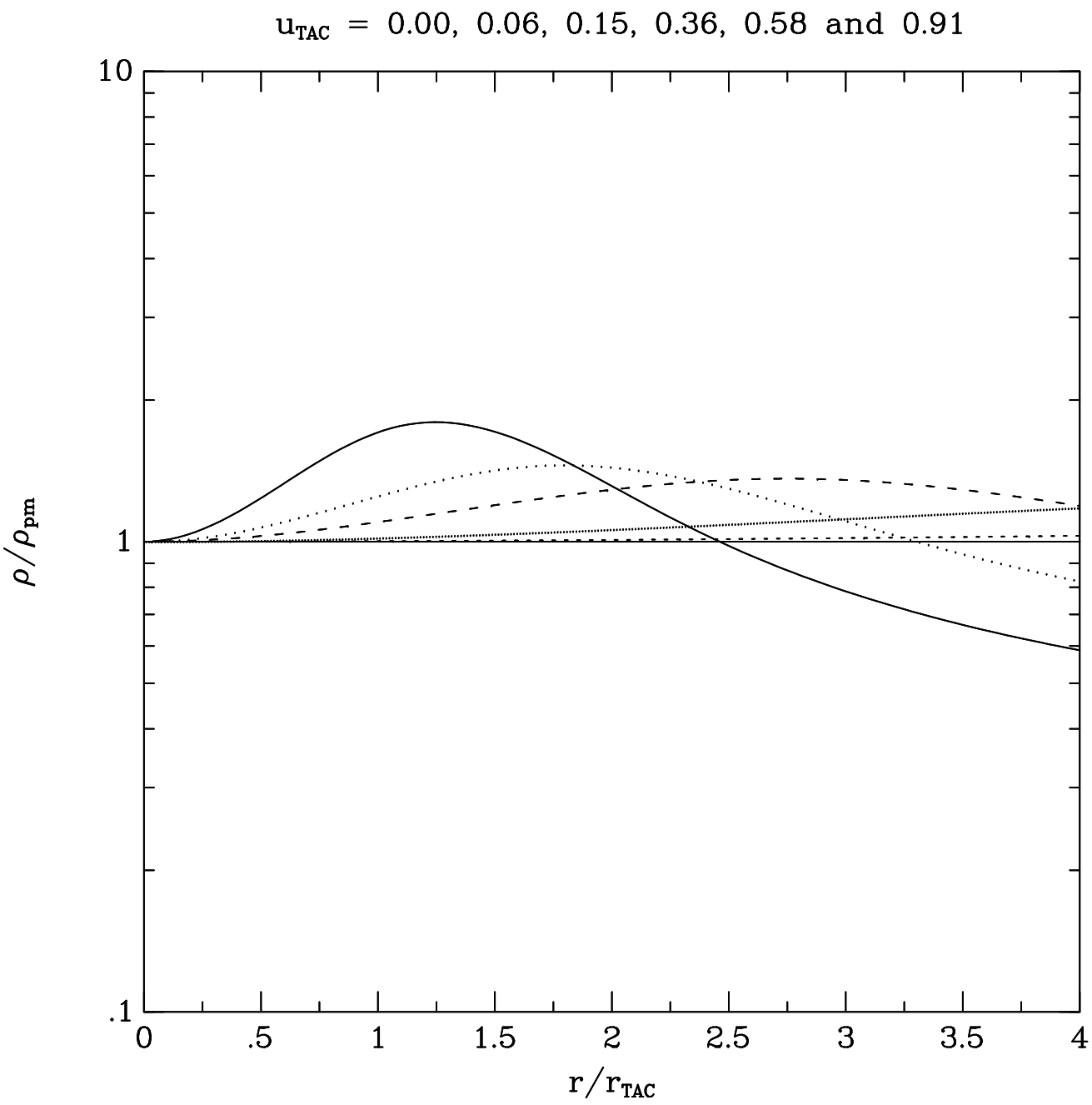
u_{TAC} = 0.00, 0.06, 0.15, 0.36, 0.58 and 0.91
10
1
.1
ρ/ρ_{pm}
0
.5
1
1.5
2
2.5
3
3.5
4
r/r_{TAC}

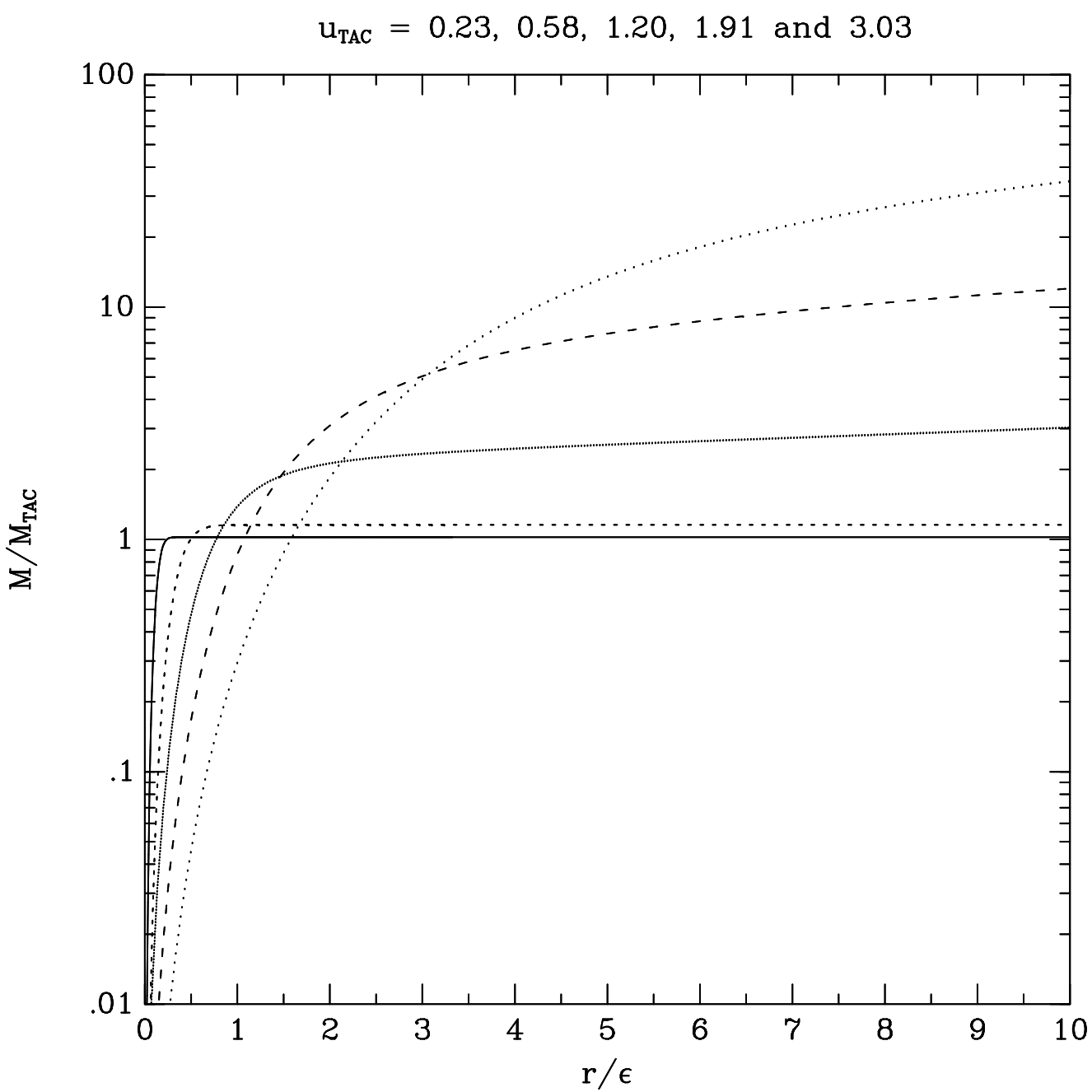
u_{TAC} = 0.23, 0.58, 1.20, 1.91 and 3.03
100
10
1
.1
.01
M/M_{TAC}
0
1
2
3
4
5
6
7
8
9
10
r/ϵ

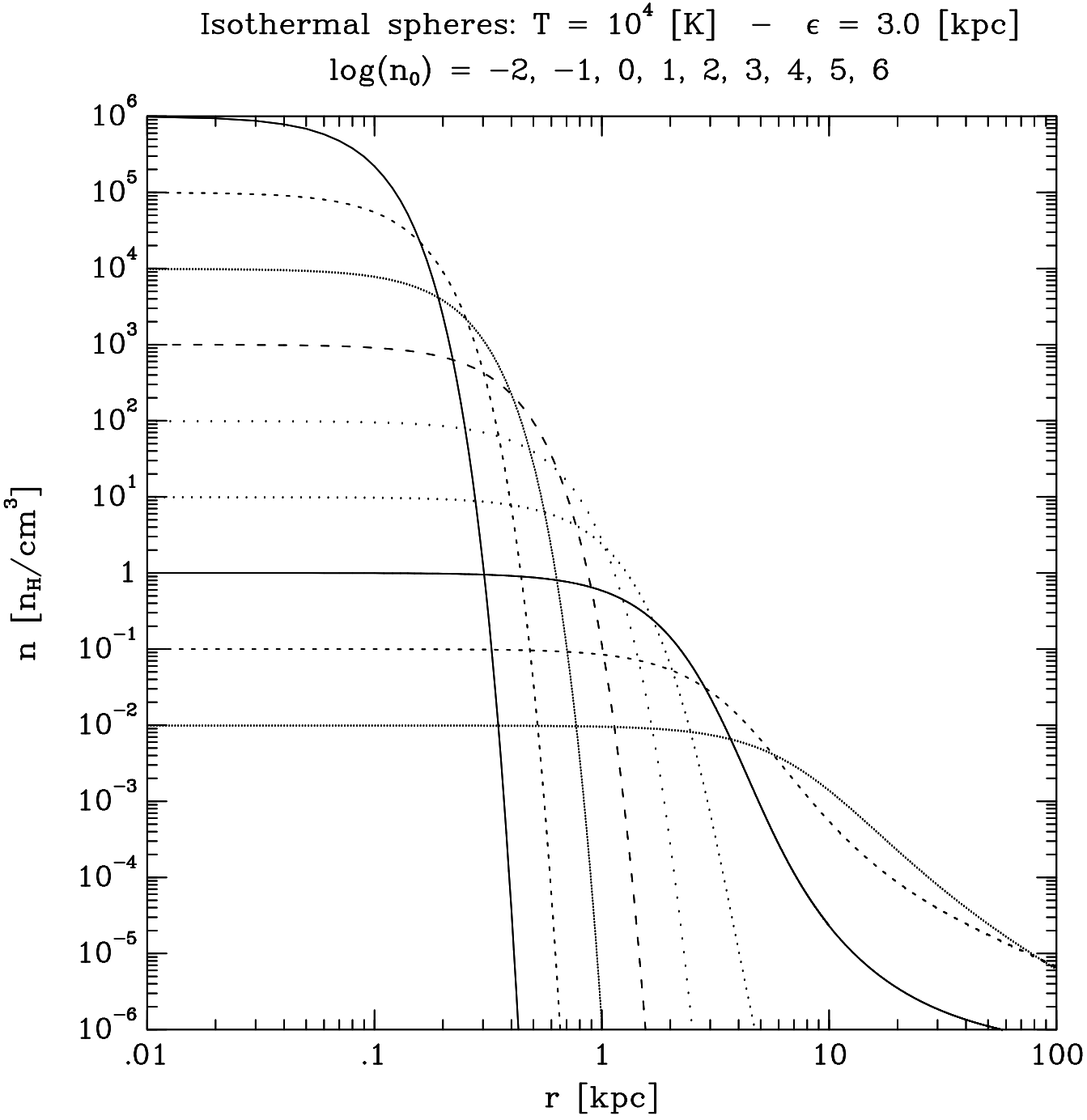
Isothermal spheres: T = 10^4 [K] − ϵ = 3.0 [kpc]
log(n0) = −2, −1, 0, 1, 2, 3, 4, 5, 6
n [nH/cm^3]
r [kpc]
10^6
10^5
10^4
10^3
10^2
10^1
1
10^-1
10^-2
10^-3
10^-4
10^-5
10^-6
.01
.1
1
10
100

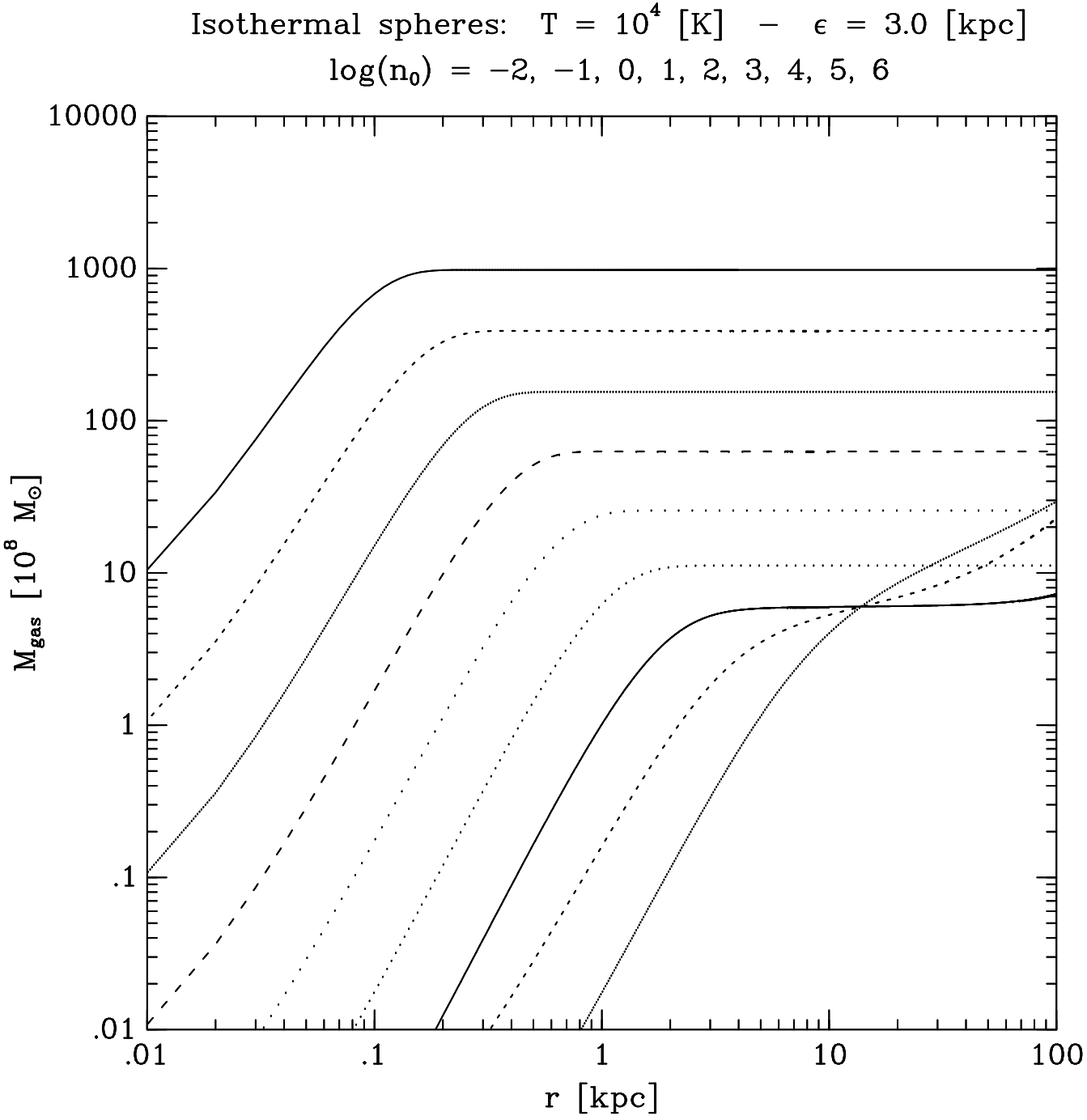
Isothermal spheres: T = 10^4 [K] − ϵ = 3.0 [kpc]
log(n0) = −2, −1, 0, 1, 2, 3, 4, 5, 6
10000
1000
100
10
1
.1
.01
Mgas [10^8 M⊙]
.01
.1
1
10
100
r [kpc]

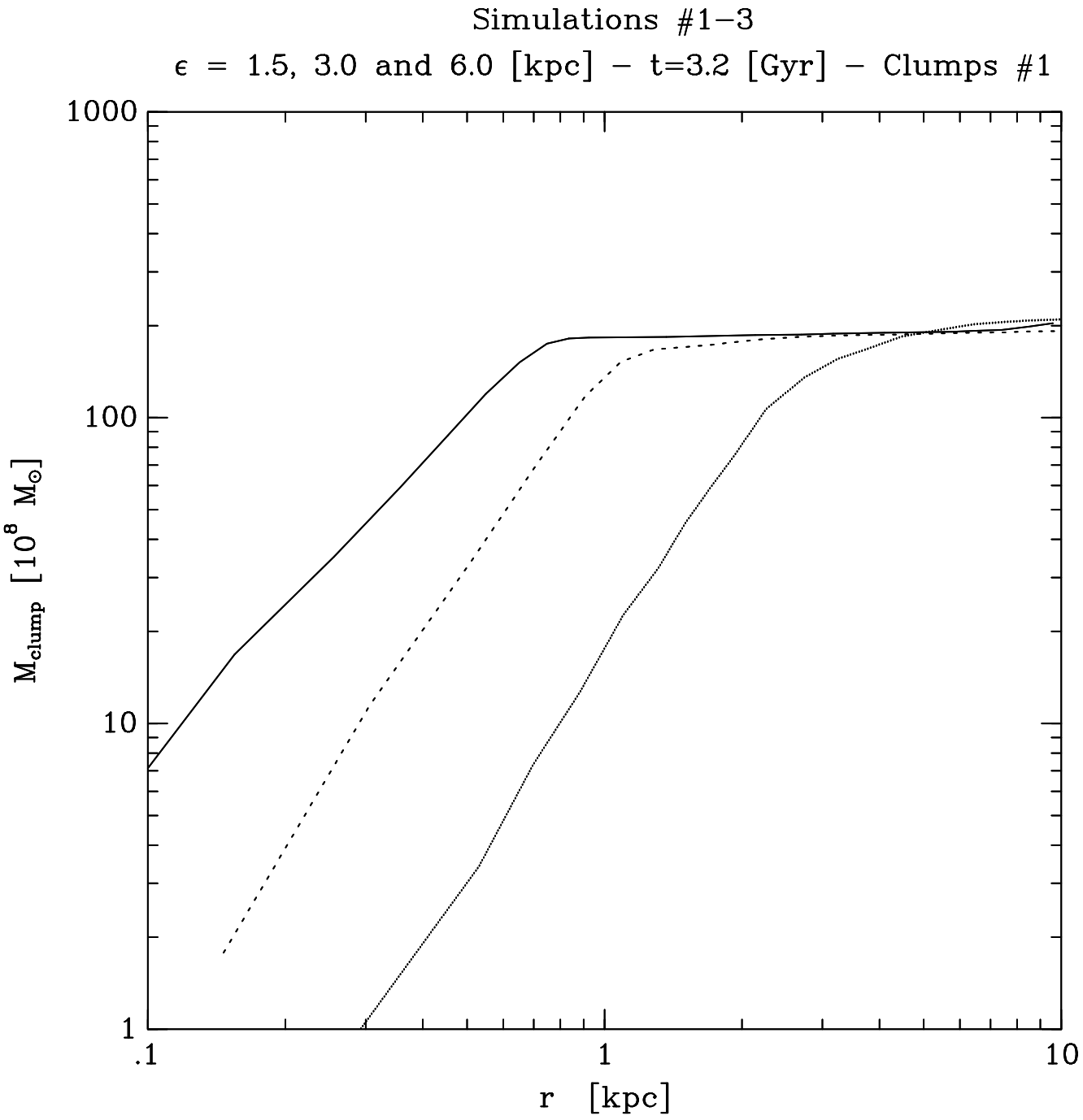
Simulations #1−3
ϵ = 1.5, 3.0 and 6.0 [kpc] − t=3.2 [Gyr] − Clumps #1
1000
100
10
1
.1
1
10
M_clump [10^8 M_⊙]
r [kpc]

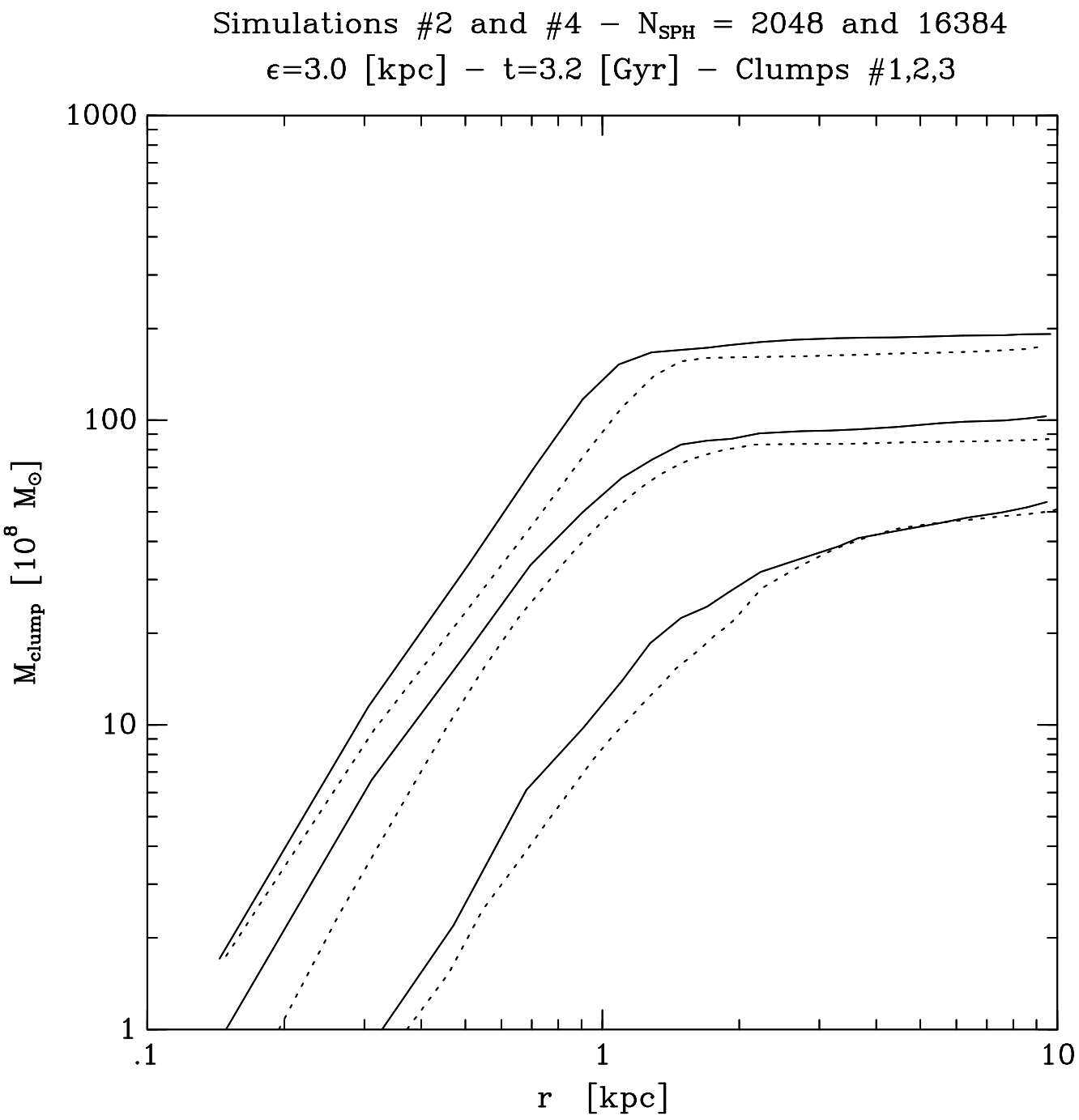
Simulations #2 and #4 – N_SPH = 2048 and 16384
ϵ=3.0 [kpc] – t=3.2 [Gyr] – Clumps #1,2,3
1000
100
10
1
.1
1
10
M_clump [10^8 M_⊙]
r [kpc]

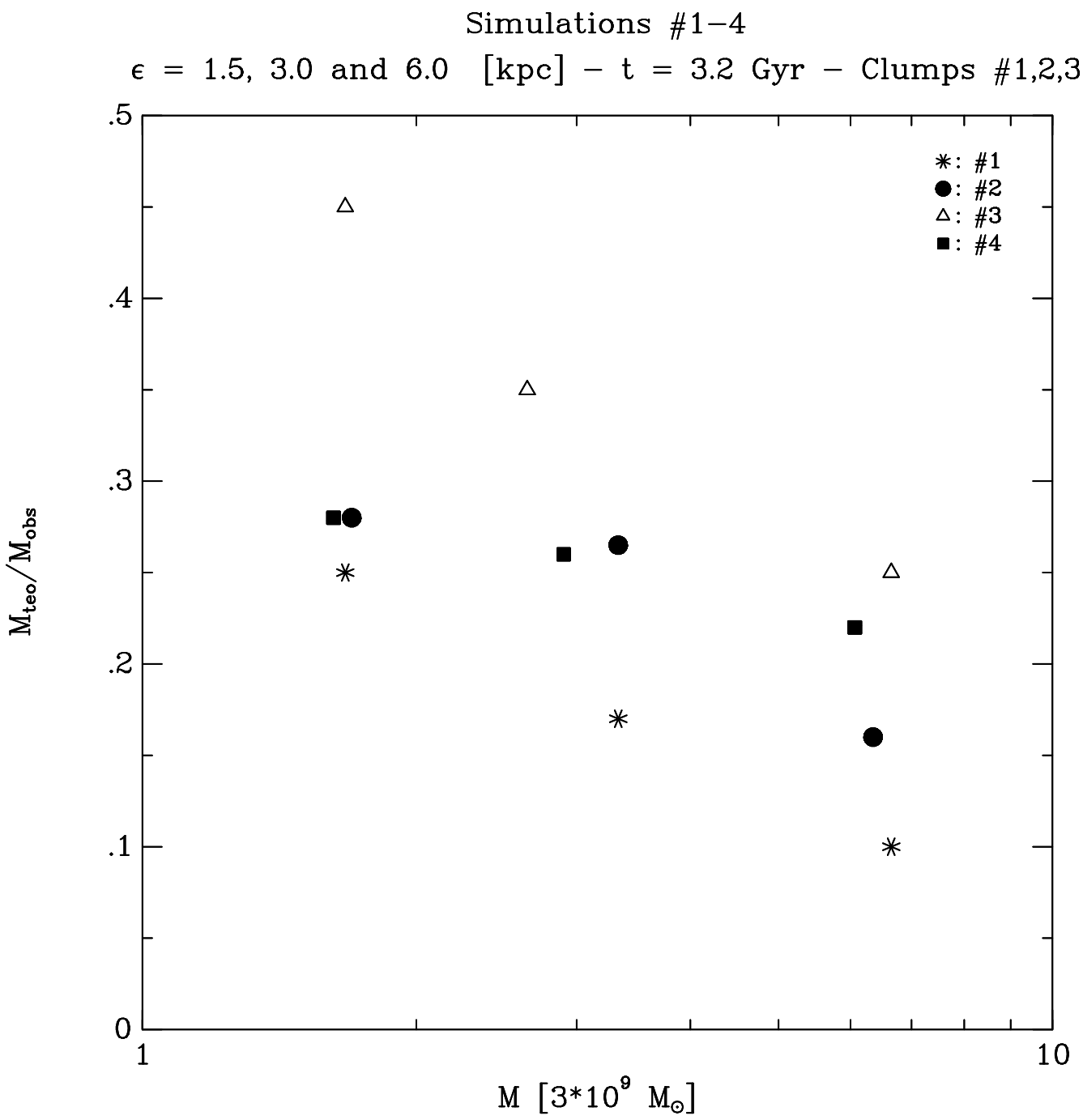
Simulations #1−4
ϵ = 1.5, 3.0 and 6.0 [kpc] − t = 3.2 Gyr − Clumps #1,2,3
.5
.4
.3
.2
.1
0
1
10
M [3*10^9 M⊙]
M_teo/M_obs
✳: #1
●: #2
△: #3
■: #4

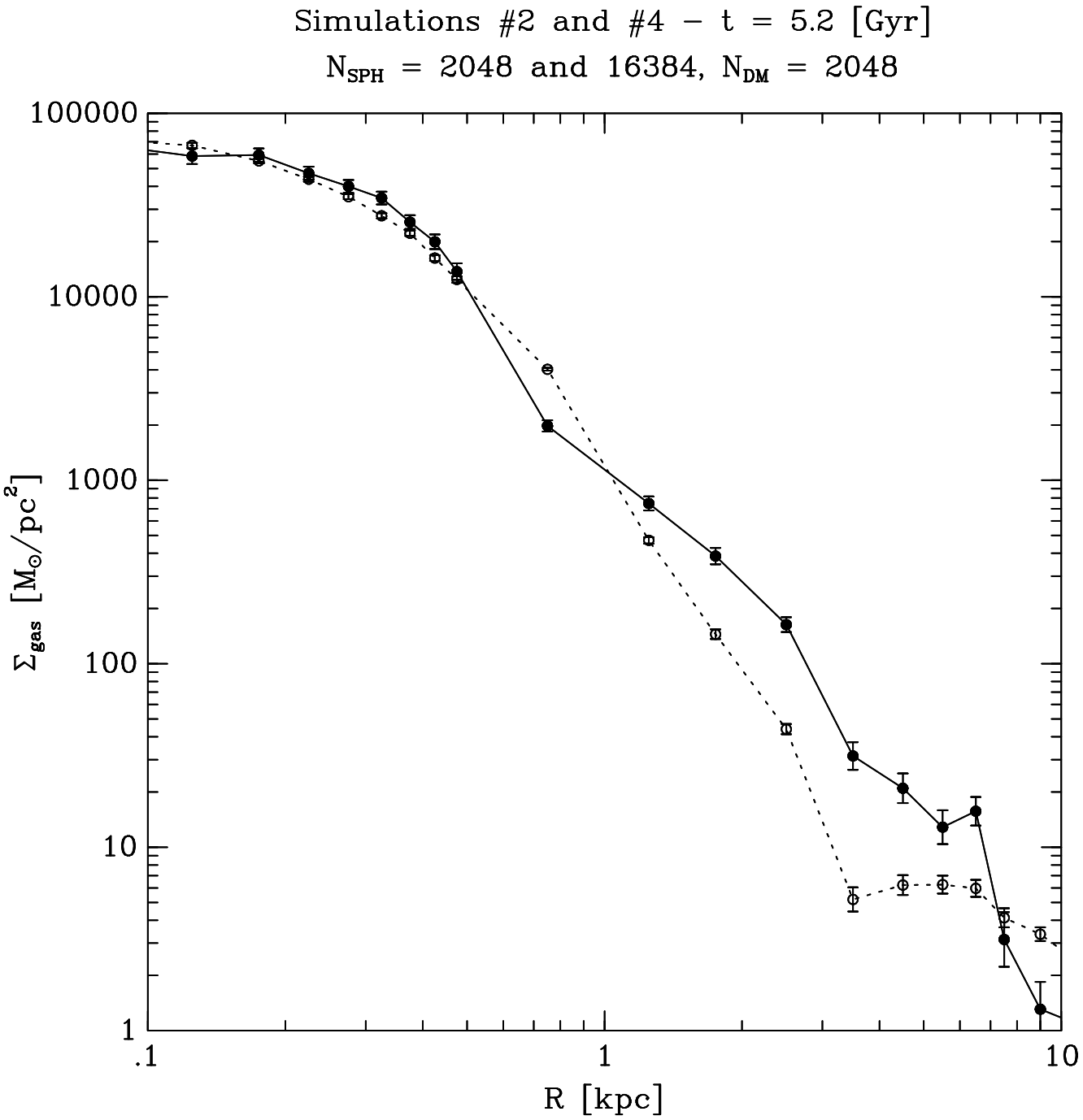
Simulations #2 and #4 – t = 5.2 [Gyr]
N_SPH = 2048 and 16384, N_DM = 2048
100000
10000
1000
100
10
1
.1
1
10
Σ_gas [M_⊙/pc^2]
R [kpc]